Estimating Inter- and Intra- Seasonal Changes of Satellite NDVI and LAI over Kherlen River Basin Using a Bi-Directional Reflectance Correction

Matsushima, D.[1], Y. Matsuura[1], I. Byanbakhuu[2], Ts. Adyasuren[2]
[1] Department of Geophysics, Tohoku University, Japan, [2] ECO Asia, Mongolia,

Keywords: bi-directional reflectance, satellite, remote sensing, NDVI, LAI

Introduction

Phenology of earth surface vegetation has been monitored by various types of spectral sensors on many satellite platforms, and the data has been being stocked over a few decades. The amount of vegetation is quantified by various spectral indices, in particular, normalized difference vegetation index (NDVI), which utilize remarkable difference of reflectance between visible (VIS) and near-infrared (NIR) bands. NDVI is simple and widely used for mapping regional distribution of vegetation growth and plotting temporal changes at various locations. Yet, NDVI has many problems, such that reflectance of soil surface under vegetation canopy has values of NDVI raised higher owing to the reflectance of soil surface in NIR band being higher than that of VIS band. Another reason which contaminates values of NDVI is caused by viewing angle of a satellite sensor. Almost all of materials covering earth surface have characteristics of reflectance which depends on the viewing angle of a sensor and the solar zenith angle, and the uniform characteristic of reflectance, called the Lambertian surface, is merely found. This kind of angular characteristic is called bi-directional reflectance. Preceded studies has experimentally showed bi-directional distributions of surface reflectance (e.g. Kimes et al., 1983), developed several models of bi- directional distribution functions (BRDF) over uniform surface (e.g. Roujean et al., 1992), verified the models using experimental data under certain conditions (e.g. Susaki, 2004), and a BRDF model is applied to the routine algorithm estimating earth surface albedo based on Moderate resolution satellite (MODIS) data (Strahler et al., 1999). However, the routine model algorithm recognizes neither the detailed classification of, nor regional distribution of vegetation types. This study shows that regional and temporal distribution of MODIS NDVI modified by a BRDF model, which is verified by field experimental data obtained during the intensive observation periods of the project of rangeland (RAISE) in years 2003 and 2004. Performance of the adjustment of NDVI using this scheme is good enough to recognize growth and dormant stages in inter- and intra- seasonal change, which are influenced by air temperature and precipitation. Without the BRDF adjustment, signal to noise ratio in some periods between growth and dormancy is not high enough to recognize the change of vegetation growth phase.

Remote Sensing Data

In this study, an archive of satellite data, which is NASA-EOS/MODIS L1B data, are used. This archive consists of 36 channels of visible and near-infrared reflectance, and thermal-infrared radiance. Spatial resolution is about 1km, and the frequency is one or two times in one daytime. The data in need are readily collected from the MODIS web server. In this study, the MODIS data are used for estimating NDVI, leaf area index (LAI).

Airborne observations were carried out in the intensive observation periods between May and October 2003. A FieldSpec, visible and near-infrared spectro-radiometer, was installed on an aircraft AN-2. The spectro-radiometer viewed steppe and forest surface in nadir angle out of the aircraft bottom window with a field-of-view of 18 deg. The flight path was a route connecting Ulaanbaatar and the RAISE observing stations.

The FieldSpec was also used in ground-based observations, which carried out bi-directional reflectance spectrometry over a steppe, a forest canopy, some water surfaces. The overall band of wavelength is between 350- 2500nm, and the resolution of wavelength is 10nm. The observations were performed in daytime almost within 9-19h local time. Duration time of a series of observation took about 20 minutes which depended on solar conditions. 90 effective series of data were obtained in the intensive observation periods in 2003 and 2004, and 85 of which were obtained over steppe and bare soil, and others over the forest site. The

procedure of a series of surface reflectance observation is as follows: (1) Surface reflection radiance viewed in a field-of-view of

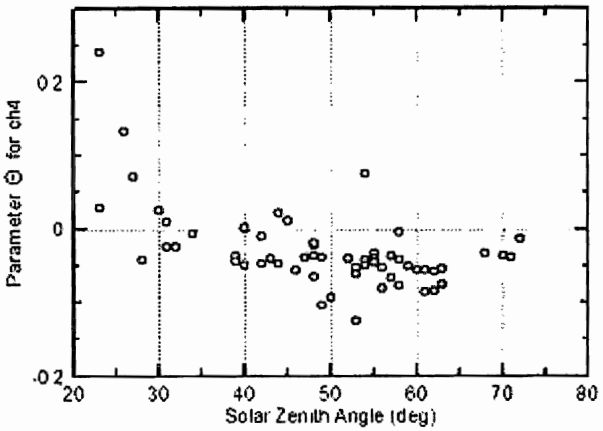

Fig. 1 Parameter Θ of the Rahman model for ch4 of MODIS as a function of solar zenith angle.

8deg (sometimes 18deg) is measured in nadir view, 8 azimuth angles (solar direction and every 45deg from the solar direction) in each diagonal angle (30, 50, and 70deg from nadir). (2) The reflectance of each measurement is calculated as the reflection radiance divided by solar hemispherical flux. An example of observed bi-directional reflectance is referred to Matsushima et al. (2005).

Bi-directional Reflectance Model

There have been several models for bi-directional reflectance distribution function. In this study, a model developed by Rahman et al. (1993) is adopted, which is formulated as follows:

$$\rho(\theta_s,\theta_v,\phi) = \rho_0 \frac{\cos\theta_s^{k-1}\cos\theta_v^{k-1}}{(\cos\theta_s+\cos\theta_v)^{1-k}} F(g)[1+R] \quad (1)$$

$$F(g) = \frac{1-\Theta^2}{[1+\Theta^2-2\Theta\cos(\pi-g)]^{1.5}} \quad (2)$$

and

$$R = \frac{1-\rho_0}{1+[\tan^2\theta s+\tan^2\theta v-2\tan\theta s\tan\theta v\cos\phi]^{\frac{1}{2}}} \quad (3)$$

$$g = \cos\theta_s\cos\theta_v+\sin\theta_s\sin\theta_v\cos\phi \quad (4)$$

where ρ is reflectance of solar zenith angle θ_s and viewing zenith angle θ_v, and viewing azimuth angle from solar direction clockwise ϕ, R expresses the hot spot effect which is extremely high reflectance at around counter side of the sun. Three unknown parameters

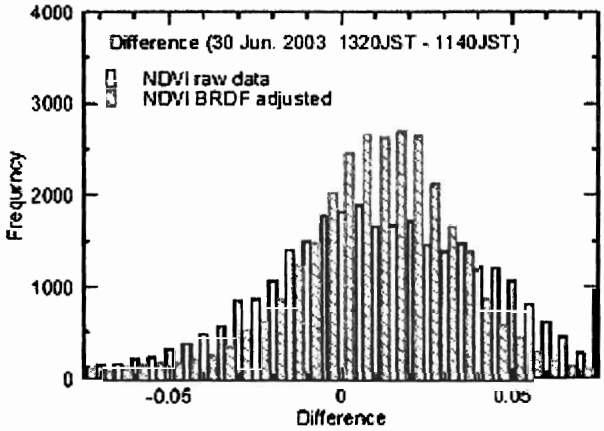

Fig. 2 Frequency histograms of difference in NDVI between two MODIS data 1140h and 1320h JST, 30 Jun. 2003.

ρ_0, Θ, k have to be determined according to respective conditions. In this study, these parameters are determined according to the ground-based data obtained over steppe and bare soil for two bands concerned with NDVI. The NDVI definition used in this study is given as

$$NDVI = \frac{NIR(ch4,adj)-VIS(ch1)}{NIR(ch4,adj)+VIS(ch1)} \quad (5)$$

where $VIS(ch1)$ is reflectance of the band of MODIS ch1 (620-670nm), $NIR(ch4,adj)$ to the band of MODIS ch4 (841-876nm) but adjusted by this formula given as

$$ch4_{adj} = ch4 - \frac{ch6-ch1}{\lambda_{ch6}-\lambda_{ch1}}(\lambda_{ch4}-\lambda_{ch1}) \quad (6)$$

where $\lambda_{ch1}, \lambda_{ch4}, \lambda_{ch6}$ are the center wavelength of each band, 645, 858, 1640nm, respectively. This adjustment is partly effective to reduce soil reflectance contamination over a specific site, but this should be further investigated. The Eq.(6) is used for calculating NDVI in the followings. Specific values of determined parameters are listed in Table 1, and the distribution of parameter Θ versus solar zenith angle is shown in Fig. 1. All parameters are well parameterized by the solar zenith angle. An example of the performance of the model is illustrated in Fig. 2. This shows histograms of NDVI calculated from two snapshots of MODIS image which captured at the same day but slightly different times. The values of NDVI should be almost the same, but in reality wide distribution of difference of raw NDVI isfound, which is caused by difference of viewing angles. On the other hand, the histogram

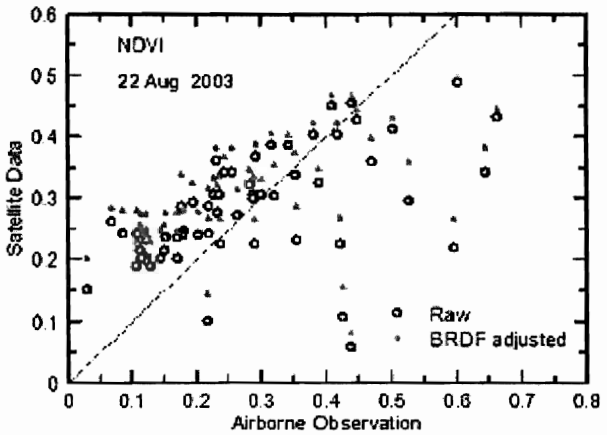

Fig. 3 Comparison of raw and BRDF adjusted NDVI estimated from simultaneous airborne and satellite observations

distribution of the adjusted NDVI is narrower, which shows the model performs fairly well. Figure 3 shows raw and adjusted NDVI estimated from the airborne and satellite observations. The satellite NDVIs, which are mostly larger than the airborne NDVIs, are fairly adjusted bur still the satellite NDVIs are a little larger. The satellite viewing angle was around 50deg from nadir in this case.

Relation between NDVI and LAI

This bi-directional adjustment method for NDVI is applied to the ground-based data, and a relation between NDVI and LAI is investigated. Figure 4 shows raw and adjusted NDVIs of ground-based data measured in various angles as a function of LAI which was measured in the RAISE project. This figure shows the plots of the adjusted NDVI and LAI are distributed roughly around the 1:1 line. Considering the accuracies of the measurements of spectral reflectance and LAI, this should be said:

$$LAI \approx \text{adjusted } NDVI \qquad (7)$$

can be applied over steppe region, provided the condition $0 <$ adjusted $NDVI < 0.7$ is satisfied. The Eq.(7) is transformed to

$$LAI \approx \text{adjusted } NDVI - 1 \qquad (7)'$$

if Eq.(6) is not used.

Intra- and Inter Seasonal Change in NDVI

Comparison of raw and BRDF adjusted NDVI from the ground-based observations as a function of LAI.

satellite NDVI based on MODIS reflectance data, in which the adjustment method for NDVI is applied. Figure 5 illustrates time series of raw and adjusted NDVI at the Kherlen-Bayan Ulaan (47d12m N, 108d44m E) and the forest stations (48d21m N, 108d36m E). The NDVIs in these figures are interpreted as LAI using Eq.(7). Both figures show the inter-seasonal change in NDVI which may be affected by the annual changes of

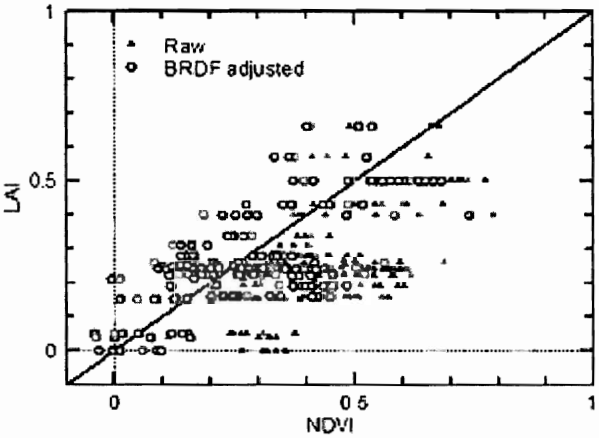

temperature. The time series of KBU also shows intra-seasonal changes in NDVI, which is like a pattern of a sudden raise followed by an exponential decrease. This pattern is well correlated with the change of soil moisture in shallow layer which is also plotted in the same figure. The remarkable thing is that this pattern look clearer in the time series of adjusted NDVI than the raw one because the S/N ratio is worse in the raw one due to the diversity of satellite viewing angles. On the other hand, the adjusted NDVIs are diverse while absolute values of them are around or less than 0.1, when the raw one are almost constant, which shows absence of green leaves. In the time series of the forest station, the intra-seasonal change found in that of KBU cannot be seen because the woods may rely on water stored in deeper soil layer where the soil moisture may not affected by short term droughts, and the forest sites is often overclouded to prevent the satellite from looking down the surface, which did not result sufficient samplings.

Summary and Future Issues

This study shows the feasibility of bi-

directional reflectance model which can be applied to ground-based observations and satellite data, which contributes to find intra-seasonal change of NDVI precisely. However, currently the feasibility is limited to the growing stages of phenology and large errors occurred in the period of absence of green leaves. These problems should be further investigated as well as raising accuracy of the relation betwen NDVI and LAI.

Acknowledgments

This study is carried out as a study of the JST-CREST/RAISE project. Dr. Saandar and MIAT Co., Ltd. totally supported the airborne observations. Staffs and students of the ECO ASIA team has greatly helped our ground-based observations.

References

Kimes, D. S., Dynamics of directional reflectance factor distribution for vegetation canopies, *Appl. Opt.*, 22, 1364-1372, 1983.

Rahman H., M. M. Verstraete, and B. Pinty, Coupled surface-atmosphere reflectance (CSAR) model, 1. Model description and inversion on synthetic data, *J. Geophys. Res.*, 98, 20779-20789, 1993.

Roujean J.-L., M. Leroy, and P.-Y. Deschamps, A bidirectional reflectance model of the Earth's surface for the correction of remote sensing data, *J. Geophys. Res.*, 97, 20455-20468, 1992.

Strahler, A. H., J.–P. Muller, and MODIS science team members, MODIS BRDF/albedo product: Algorithm theoretical basis document version 5.0, 1999.

Susaki, J., K. Hara, K. Kajiwara, and Y. Honda, Robust estimation of BRDF model parameters, *Remote. Sens. Env*, 89, 63-71, 2004.

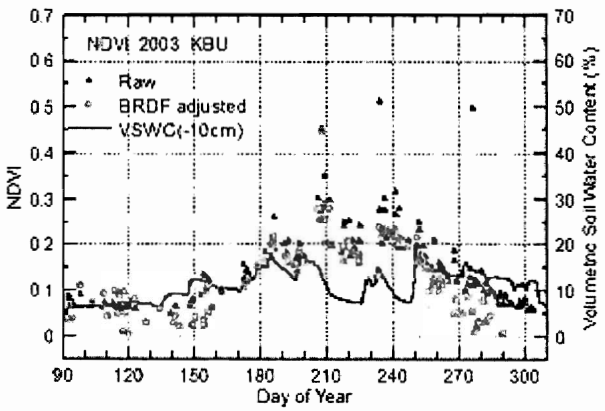

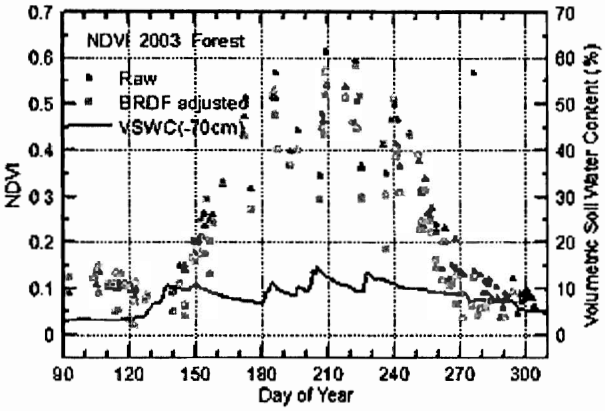

Table 1 Parameters of Eqs.(1)-(3).

ρ_0

Ch1 $0.001(62-\theta_s)$, $20 < \theta_s < 45$ deg
0.017, $45 < \theta_s$

Ch2 $0.002(70-\theta_s)$, $20 < \theta_s < 50$ deg
0.04, $50 < \theta_s$

Ch3 $0.0004(70-\theta_s)$, $20 < \theta_s < 47$ deg
0.01, $47 < \theta_s$

Ch4 $0.001(60-\theta_s)$, $20 < \theta_s < 47$ deg
0.013, $47 < \theta_s$

Ch5 $0.0024(70-\theta_s)$, $20 < \theta_s < 45$ deg
0.06, $45 < \theta_s$

Ch6 $0.003(68-\theta_s)$, $20 < \theta_s < 50$ deg
0.054, $50 < \theta_s$

k

Ch1 0.75 Ch4 0.7
Ch2 0.65 Ch5 0.75
Ch3 0.7 Ch6 0.8

Θ

Ch1(620-670nm), 3(459-479nm), 4(545-565nm)
$0.03(30-\theta_s)$, $20 < \theta_s < 30$ deg
$0.005(30-\theta_s)$, $30 < \theta_s < 40$ deg
-0.05, $40 < \theta_s$ deg

Ch2(841-876nm), 5(1230-1250nm), 6(1628-1652nm)
$0.03(30-\theta_s)$, $20 < \theta_s < 30$ deg
$0.01(30-\theta_s)$, $30 < \theta_s < 40$ deg
-0.1, $40 < \theta_s$ deg